J Fusion Energ (2014) 33:707–712
DOI 10.1007/s10894-014-9735-0

ORIGINAL RESEARCH

The Simulation of Certain Properties of Plasma Affecting Beam-Driven Current in EAST

Ji Wang · Bin Wu · Jinfang Wang · Chundong Hu

Published online: 2 July 2014

Abstract Some properties of plasma are investigated for the impact of the beam-driven current in experimental advanced superconducting tokamak (EAST). Beam-driven current simulation experiments have been performed to study beam-driven current due to the density, temperature and Z_{eff} of plasma for the on-axis injection. These impact factors for the co-injection and counter-injection are considered qualitatively and quantitatively under some certain specified experimental conditions to guide the future EAST experimental campaign.

Keywords EAST · Neutral beam · Beam-driven current · Plasma

Introduction

The method of producing current generated by tangential neutral beam injection (NBI) in a tokamak was first proposed by Ohkawa [1], and then the beam-driven current was first observed in the Culham Laboratory Levitron [2]. The toroidal plasma current is indispensable to sustaining plasma equilibrium in a tokamak configuration during discharging. The NBI, as one of the important non-inductive current drive methods, is applied to change the plasma loop voltage because the Ohmic heating transformer circuit maintains the total current approximately constant. When the beam injection is in the direction of the Ohmic current, namely co-injection, some of the latter is replaced by the beam-driven current and the loop voltage is reduced accordingly. For counter-injection, the opposite occurs [3].

A positive-ion-based on-axis NBI system of the experimental advanced superconducting tokamak (EAST) has been installed recently on Window A and is well prepared for the next EAST experimental campaign. The next beamline on Window F for counter-injection is being constructed. The layout of the NBI system location is shown in Fig. 1. The same two ion sources are included in each beamline, and the angle between the two beams on the same window is 8.7°. The maximal designed power and energy of each beamline are 4 MW and 80 keV. Some important beam capability indices are also adjustable in a certain range.

For a specific beam injection, the factors impacting the efficiency of beam-driven current are too many. In the following we will mainly discuss certain target plasma conditions which can influence the beam-driven current in EAST by simulation using a 1.5D transport code ONETWO [4] and a Monte Carlo code NUBEAM [5].

The beam-driven current is given by the sum of the beam ion current and the retarding current produced by electrons flowing in the same direction as the beam. The retarding current is basically determined by the electron force balance of acceleration by the collision with beam ions and deceleration by the collisions with bulk ions [6].

For toroidal plasma, the motion of circulating electrons is disturbed by collision with the trapped electrons, and then the term of retarding electrons is reduced. Then the beam-driven current is given by

$$I_{beam} = I_{ion} + I_{r\_elec} = I_{ion}\left[1 - \frac{Z_b}{Z_{eff}}(1 - G)\right] \tag{1}$$

where I_{ion}, I_{r_elec}, Z_b, Z_{eff} and G are beam ion current in plasma, retarding current due to electrons, ionic charge

J. Wang (✉) · B. Wu · J. Wang · C. Hu
Institute of Plasma Physics, China Academy of Sciences, Hefei 230031, People's Republic of China
e-mail: wangji@ipp.ac.cn

Fig. 1 Configuration of NBI on EAST

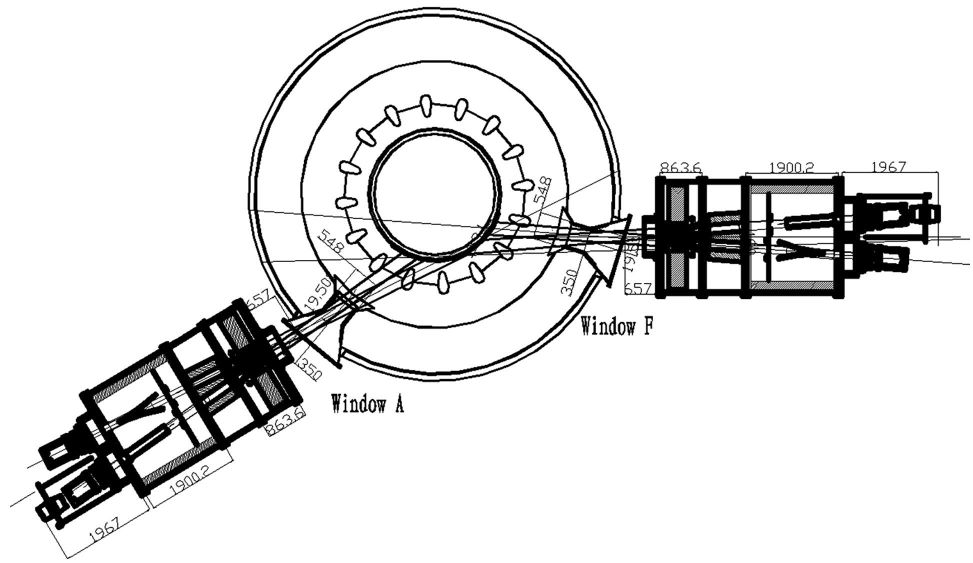

number of beam, effective ionic charge number of plasma, and geometrical factor respectively. The physical meaning of the geometrical factor G is related with trapped and non-trapped electrons, and depends on the magnetic configuration [7, 8]. This formula seems to be simple to understand, but there is still difference between experimental observation and theory because of the geometrical factor G which is still rather hard to express clearly due to the complicated physics. Further developed theories were proposed in succession and all these theories considered some corrections based on Eq. (1) [9–12].

In this paper, certain impact factors of EAST plasma on beam-driven current are considered and analyzed in Sect. 2 and the total toroidal current is kept at 0.98 MA in all simulative experiments for convenient comparison.

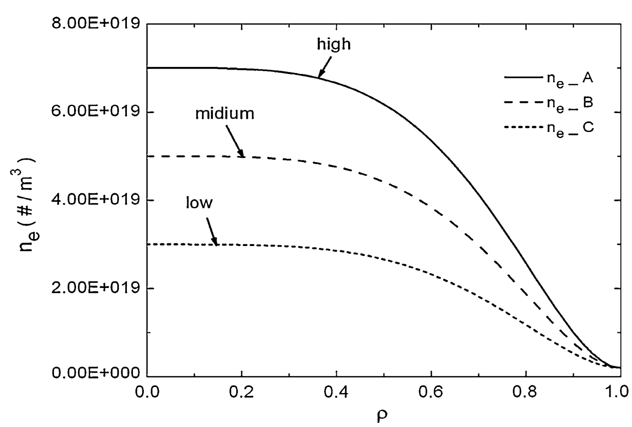

Fig. 2 Three different plasma density profiles are considered in these simulative experiments and each keeps stable with Te(0) = Ti(0) = 3.0 keV at the magnetic axis during the NBI on EAST. The abscissa is the normalized square root of the toroidal flux

Certain Effective Properties of Plasma Affecting Beam-Driven Current

Different Plasma Density

The energetic beam atoms injected into the tokamak become ionized through collisions with the plasma particles and the resulting ions and electrons are then held by the magnetic field. It's obvious that the ionization is affected by the target plasma density. The experiments on EAST are being promoted to high specifications and the plasma density is an important one of them. Here different density profiles, namely high, medium and low density distribution shown in Fig. 2, are considered for contribution to the beam-driven current during NBI on EAST.

The beam-driven current profiles under the full power and energy conditions of power 4 MW, beam energy 80 keV with co- and counter-injection respectively are shown in the Fig. 3, and the integral contributions are shown in Fig. 4.

The three density profiles in the simulation are carefully selected to avoid too low density for beam shine-through and less ionization to produce little beam-driven current. The beam-driven current density is higher in the core, and the outside is lower. It can be seen that the lower density leads to higher beam-driven current efficiency. This result can't be clearly concluded from Eq. (1), but given the inverse aspect ratio, pitch angle, bounce average and other corrections, the beam drive efficiency is proportional to I_{ion}/n_e [9, 13]. In these simulative experiments, high

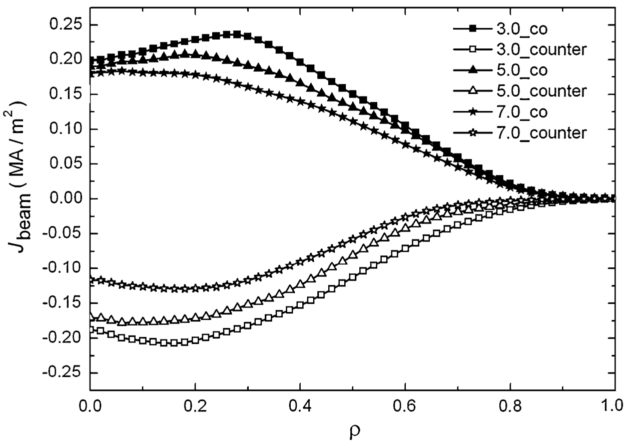

Fig. 3 Different beam-driven profiles with co- and counter-injection in three different plasma density during NBI

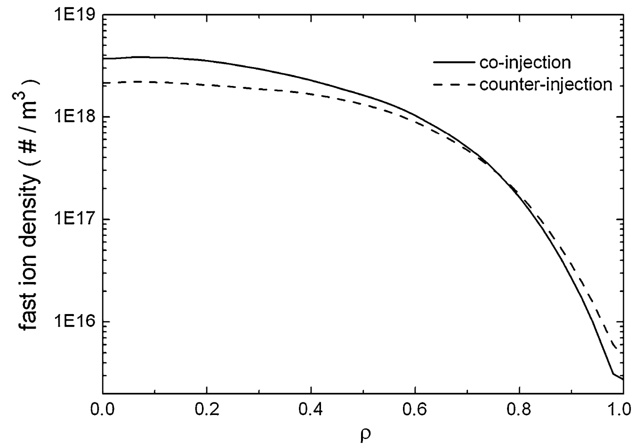

Fig. 6 Fast ions density profiles of co- and counter-injection with the medium plasma density in Fig. 2

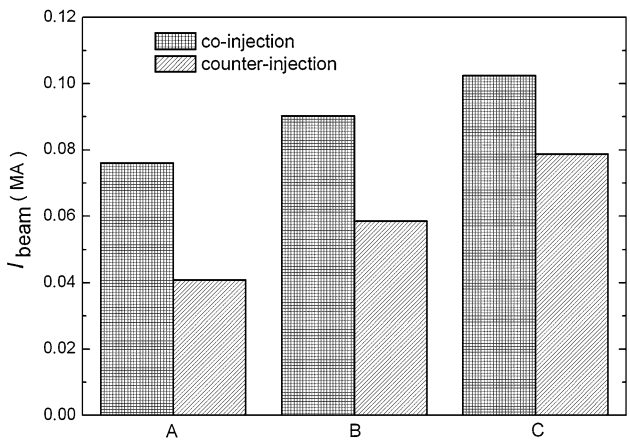

Fig. 4 The total beam-driven contributions with co- and counter-injection are indicated with *bars*. Here, the absolute value of counter-injection beam-driven current (*light shadow*) is shown for convenient comparison with co-injection contribution

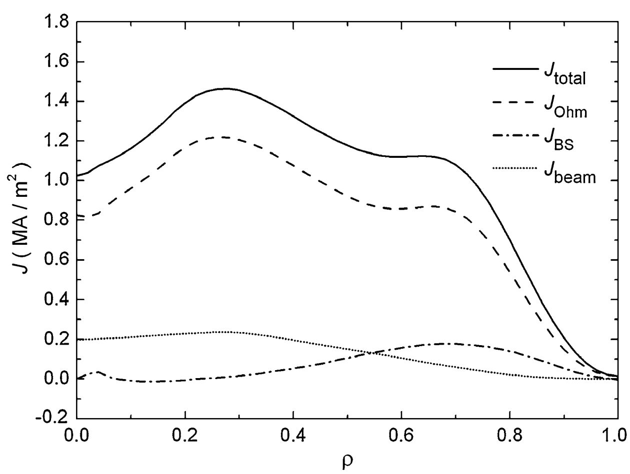

Fig. 5 Radial profiles of total (J_{total}), Ohmic (J_{Ohm}), bootstrap (J_{BS}) and NB (J_{beam}) current with 4 MW and 80 keV beam co-injection into the low density shown as Fig. 2

density results in more collision and ionization probability between beam atoms and bulk ions, so I_{ion} increases with the increasing n_e. From the results, we also find that the increased I_{ion} is not proportional to the increased n_e, and the former is smaller than the latter. For this reason, the beam-driven current with density 7.0 × 10^{19}/m^3 (at magnetic axis) is lower than that with density 3.0 × 10^{19}/m^3 (at magnetic axis).

We can see that the maximal beam-driven current in these cases is 0.11 MA, and this value is rather small compared with the total current 0.98 MA. The current profiles in this case are illustrated in Fig. 5.

In this case, $J_{tatal} = J_{Ohm} + J_{BS} + J_{beam}$. It shows that the Ohmic current is the largest share of total current, and beam-driven current only accounts for 11 % although it reaches the maximal value in these cases. If the total current is reduced in other scenarios, the beam-driven current will increase its share and remarkably leads to a reduction of the loop voltage.

The beam-driven current efficiency of co-injection is obviously higher than that of counter-injection and the difference between these two direction injections increases with the increasing density. The deference is only 0.02 MA in the low density, while the deference increases to 0.035 MA in the high density shown in Fig. 4.

There are some interpretations on this phenomena [14–17]. Besides these, we find that the fast ions profiles are also different between co- and counter-injection shown in Fig. 6.

The fast ion density of co-injection in the core is obviously higher than that of counter-injection, while in the outside, the opposite happens. The overall effect leads to more fast ion population of co-injection which is higher than that of counter-injection because there is only minor

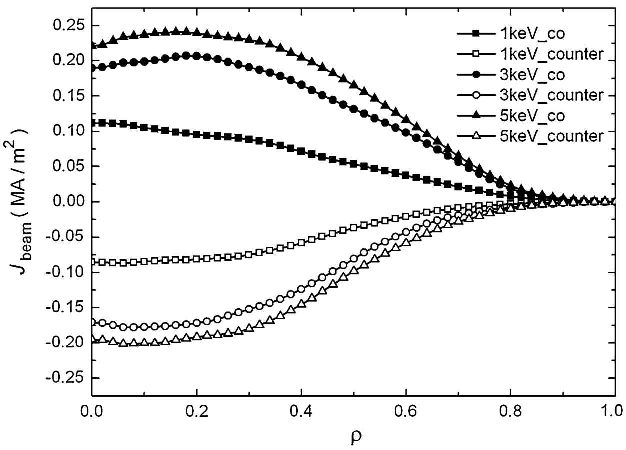

Fig. 7 Beam-driven current density profiles in three different plasma temperature with 4 MW and 80 keV beam co- and counter-injection

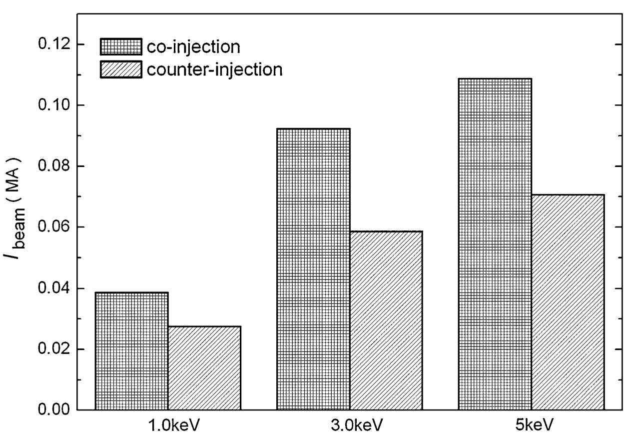

Fig. 8 Beam-driven current for different plasma temperature

difference outside the half plasma as to the order of magnitude.

Different Plasma Temperature

A neutral beam is always injected into a certain temperature target plasma, and impact ionization cross-section is related with plasma temperature. The temperature is a significant factor in the beam-driven current efficiency. In this simulation experiment, the density is shown as the medium profile in Fig. 2, and the electron and ion temperatures are supposed to be the same in the three cases, namely the core temperature is 1.0, 3.0 and 5.0 keV respectively. These radial temperature profiles are approximately similar to the density profiles shown in Fig. 2. The beam-driven current results are shown in Figs. 7 and 8.

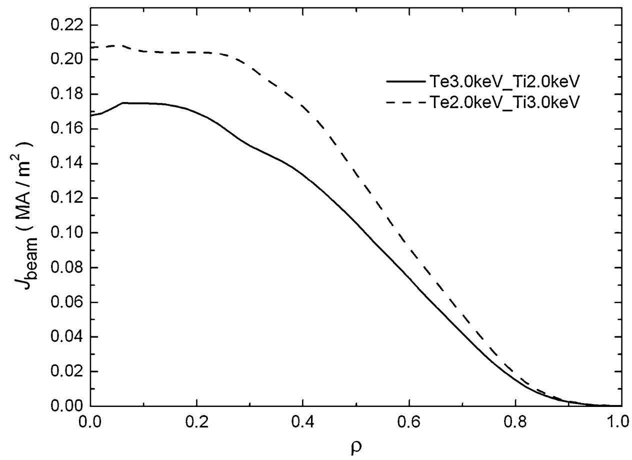

Fig. 9 Beam-driven current density in different temperature of electron and ion with 4 MW and 80 keV beam co-injection maintaining the medium density in Fig. 2

It can be seen that when the plasma core temperature is 1.0 keV the co-injection beam-driven current is just about 0.04 MA, while the current is sharply increased to about 0.11 MA when the plasma core temperature is promoted to 5.0 keV. With the increasing plasma temperature the beam-driven current efficiency is better. According to OKANO's neoclassical formula for neutral beam current drive, the beam-driven current efficiency is proportional to T_e [10]. We think that the beam-driven current is related to T_e and increases with increasing temperature, but it is not strictly proportional to T_e because the effective ionization cross-section σ_{eff} of beam atoms injected into plasma tends to be small with increasing plasma temperature when multistep excitation processes are neglected [18], and this reduced $\Delta\sigma_{eff}$ is not proportional to ΔT_e. The assumption is proven by the beam shine-through power loss in this case. When the temperature is increased from 1.0 to 5.0 keV at the core, the shine-through power increases from 0.62 to 0.73 MW. It's obviously not a linear relationship. From this point, the OKANO's formula needed to be further corrected.

Besides the above temperature experiments, different temperature of electron and ion in plasma is also investigated. At the magnetic axis $T_e = 3.0$ keV and $T_i = 2.0$ keV versus $T_e = 2.0$ keV and $T_i = 3.0$ keV is considered during NBI on EAST. The beam-dream current density is shown in Fig. 9.

In these two cases, the current drive efficiency is higher for the combination of low T_e and high T_i, and the total beam-driven current is 0.09 and 0.07 MA respectively. To compare Figs. 9 with 7 and 8 when the temperature is 3 keV, we find that lower T_e has a very minor effect on the

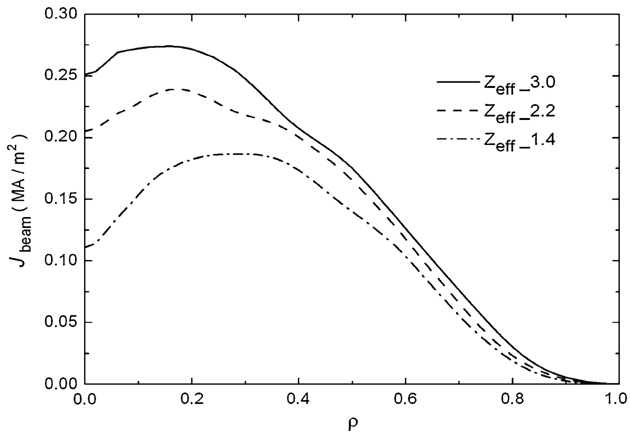

Fig. 10 Beam-driven current density profiles due to different Z_{eff}

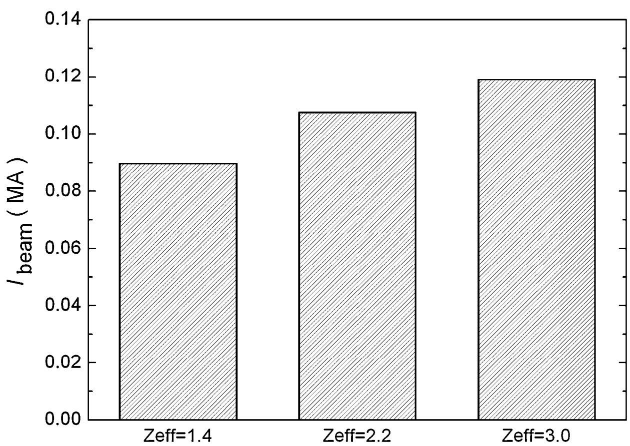

Fig. 11 Beam-driven current due to different Z_{eff}

beam-driven current, while lower T_i can result in significantly reduced current.

Different Z_{eff}

It is necessary for a nuclear tokamak to make the assumption that the cross-section for a given process depends only on the relative collision velocity [19]. It means that direct ion impact is the dominant ionization process of neutral beam in EAST, and the ionization cross-section of the neutral beam is also considered to be related to Z_{eff} in the plasma [6]. The retarding electron current is also partially determined by Z_{eff} from Eq. (1).

In this case, three uniform radial distribution profiles Z_{eff} in plasma, namely 1.4, 2.2 and 3.0 are investigated in order to simplify the analysis of the beam-driven current dependence on Z_{eff}.

The EAST density in the simulation is as the medium profile shown in Fig. 2. Te(0) = Ti(0) = 3.0 keV. The co-injected beam parameters are 80 keV and 4 MW. The beam-driven current dependences on Z_{eff} are shown in Figs. 10 and 11.

With the Z_{eff} increase, the beam-driven current effeciency is also promoted,and there are obvious differences inside the half inner plasma, while there is minor difference between them outside the half plasma. The results agree with the observed experiments conducted on DIII-D by Park [20]. The Z_{eff} effect on the beam-driven current can be clearly derived from Eq. (1). That means less retarding electron current because of more decelerating collisions between electrons and impurity ions besides bulk ions with the increased Z_{eff}. We can see that the Z_{eff} impact on the beam-driven current is not as magnificent as the plasma temperature from the integral current. This means that to achieve high beam-driven current by increasing Z_{eff} is not very effective, and exorbitant Z_{eff} may also lead to disruption during discharge.

Conclusion

Certain plasma properties affecting beam-driven current have been studied on EAST in these simulation experiments and some instructively qualitative and quantitative results can be utilized to guide the next EAST experimental campaign. The beam-driven current of co-injection is obviously higher than that of counter-injection under the same plasma and beam conditions. To reduce the target plasma density appropriately or (and) to increase the temperature can result in promoting the beam-driven current while the other experimental conditions remain basically unchanged. To increase the Z_{eff} can also promote the beam-driven current efficiency to some extent, but exorbitant impurity ions may result in disruption.

Acknowledgments We thank the National Transport Code Collaboration (NTCC) and General Atoms (GA) for their contributions to the development of tokamak and beam simulation codes. This work was supported by the National Natural Science Foundation of China (Granted Numbers 11247302 and 11175211), Ministry of Science and Technology of PRC (Granted Number 2013GB101000) and National Development and Reform Commission of PRC. We also thank Jan. Weiland for discussing and revising the content of this article.

References

1. T. Ohkawa, New methods of driving plasma current in fusion devices. Nucl. Fusion **10**, 185 (1970)
2. D.F.H. Start et al., Observation of beam-induced currents in a toroidal plasma. Phys. Rev. Lett. **40**, 1497–1500 (1978)
3. W.H.M. Clark et al., Measurements of the beam-driven current in the Dite tokamak. Phys. Rev. Lett. **45**, 1101–1104 (1980)

4. https://fusion.gat.com/THEORY/onetwo/
5. http://w3.pppl.gov/ntcc/NUBEAM
6. K. Nagaoka et al., Z dependence of neutral beam driven current in the large helical device and the compact helical system. J Korean Phys Soc **49**, S92–S95 (2006)
7. J.G. Cordey et al., Kinetic-theory of beam-induced plasma currents. Nucl. Fusion **19**, 249–259 (1979)
8. S.P. Hirshman, Classical collisional theory of beam-driven plasma currents. Phys. Fluids **23**, 1238–1243 (1980)
9. D.F.H. Start et al., Beam-induced currents in toroidal plasmas of arbitrary aspect ratio. Phys. Fluids **23**, 1477–1478 (1980)
10. K. Okano, Neoclassical formula for neutral beam current drive. Nucl. Fusion **30**, 423–430 (1990)
11. M. Taguchi, Approximate expression for beam driven current in tokamak plasmas. Nucl. Fusion **32**, 143–150 (1992)
12. Y.R. LinLiu et al., Trapped electron correction to beam driven current in general tokamak equilibria. Phys. Plasmas **4**, 4179–4181 (1997)
13. D.F.H. Start et al., The effect of trapped electrons on beam driven currents in toroidal plasmas. Plasma Phys. Controll Fusion **22**, 303–316 (1980)
14. P. Helander et al., On neutral-beam injection counter to the plasma current. Phys. Plasmas **12**, 112503 (2005)
15. D.R. Mikkelsen et al., Energetic particle orbits in the national spherical Tokamak experiment. Phys. Plasmas **4**, 3667–3675 (1997)
16. W.W. Heidbrink et al., Beam-ion confinement for different injection geometries. Plasma Phys. Controll. Fusion **51**, 125001 (2009)
17. R.J. Akers et al., Neutral beam heating in the START spherical tokamak. Nucl. Fusion **42**, 122–135 (2002)
18. E. Speth, Neutral beam heating of fusion plasmas. Rep. Prog. Phys. **52**, 57–121 (1989)
19. A.C. Riviere, Penetration of fast hydrogen atoms into a fusion reactor plasma. Nucl. Fusion **11**, 363 (1971)
20. J.M. Park et al., Validation of on- and off-axis neutral beam current drive against experiment in DIII-D. Phys. Plasmas **16**, 092508 (2009)